Optimum Space–Time Processors with Dispersive Interference: Unified Analysis and Required Filter Span

Sirikiat Lek Ariyavisitakul, *Senior Member, IEEE,* Jack H. Winters, *Fellow, IEEE,* and Inkyu Lee, *Member, IEEE*

***Abstract*— In this paper, we consider optimum space–time equalizers with unknown dispersive interference, consisting of a linear equalizer that both spatially and temporally whitens the interference and noise, followed by a decision-feedback equalizer or maximum-likelihood sequence estimator. We first present a unified analysis of the optimum space–time equalizer, and then show that, for typical fading channels with a given signal-to-noise ratio (SNR), near-optimum performance can be achieved with a finite-length equalizer. Expressions are given for the required filter span as a function of the dispersion length, number of cochannel interferers, number of antennas, and SNR, which are useful in the design of practical near-optimum space–time equalizers.**

***Index Terms*— Equalization, interference suppression, multipath channels, space–time processing.**

I. Introduction

IN WIRELESS communication systems, cochannel interference (CCI) and intersymbol interference (ISI) are major impairments that limit the capacity and data rate. These problems can be mitigated by spatial-temporal (S-T) processing, i.e., temporal equalization with multiple antennas [1]–[11].

In typical wireless systems where the cochannel interferers are unknown at the receiver, optimum S-T equalizers, either in a minimum mean square error (MMSE) or maximum signal-to-interference-plus-noise ratio (SINR) sense, consist of a whitening filter, i.e., an equalizer that whitens the CCI both spatially and temporally, followed by a decision-feedback equalizer (DFE) or maximum-likelihood sequence estimator (MLSE) [12].

However, under some channel conditions with dispersive CCI, the whitening filter requires an infinite span to achieve near-optimum performance, even with reasonable signal-to-noise ratios (SNR's). For typical fading channels, though, such channel conditions occur only occasionally, and the required filter span for near-optimum performance is finite in most cases. Since the filter span, specifically both the causal and anticausal portions, determines the required memory of the DFE and MLSE, these filter spans determine the required complexity of near-optimum S-T processors.

In this paper, we first present a unified analysis of the optimum infinite-length S-T processor, considering three receiver types: 1) MMSE linear equalizer (LE); 2) MMSE-DFE; and 3) MLSE. The unified analysis includes both previously published results [12], [17]–[19] and additional new material. The objective here is to provide a consistent and comprehensive framework for expressing all these results in a form that is descriptive of the functions and properties of individual filter elements. We then present filter length analyzes for all three receivers by analyzing the z-transform expressions. We show that, with fading channels, the filter spans of these receivers can be truncated such that the average effect of the truncation is small compared to the effect of thermal noise. We then determine the required filter span to achieve near-optimum receiver performance. These expressions for the required filter span as a function of the dispersion length, number of cochannel interferers, and SNR are useful in the design of practical near-optimum space–time equalizers. Using computer simulation, we study the effect of thermal noise on the required filter span for specific fading channels.

In Section II, the system model and notation is defined. The unified analysis is presented in Section III, and in Section IV the finite filter span analysis is presented. Section V shows numerical results. A summary and conclusions are given in Section VI.

II. System Model

We consider a system where $L+1$ cochannel signals are transmitted over independently fading multipath channels to an M-branch diversity receiver. The time-domain complex baseband expression of the received signal on the jth antenna is

$$r_j(t) = \sum_{i=0}^{L} \sum_{n=-\infty}^{\infty} x_{ni} h_{ij}(t-nT) + n_j(t) \tag{1}$$

where $\{x_{ni}\}$ is the transmitted data sequence from the ith source, with the *desired* source being indexed by $i=0$; $h_{ij}(t)$ is the overall impulse response of the transmission link between the ith source and the jth antenna; T is the symbol period; and $n_j(t)$ is the additive white Gaussian noise at the jth antenna. The data $\{x_{ni}\}$ are independently identically,

Paper approved by K. B. Letaief, the Editor for Wireless Systems of the IEEE Communications Society. Manuscript received May 20, 1998; revised October 20, 1998. This paper was presented in part at the IEEE Internaional Conference on Communications, Vancouver, BC, Canada, June 1999.

S. L. Ariyavisitakul is with Home Wireless Networks, Norcross, GA 30071 USA (e-mail: lek@homewireless.com).

J. H. Winters is with AT&T Labs-Research, Red Bank, NJ 07701 USA.

I. Lee is with Bell Labs, Lucent Technologies, Murray Hill, NJ 07974 USA.

Publisher Item Identifier S 0090-6778(99)05236-8.

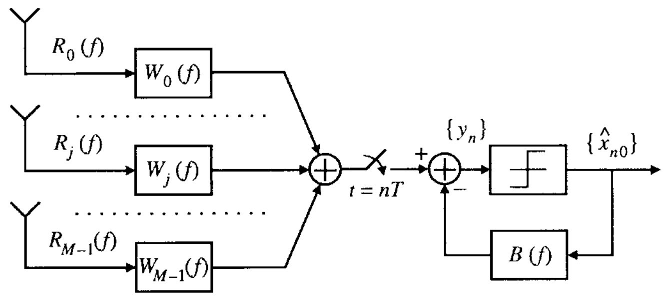

Fig. 1. A space–time DFE receiver.

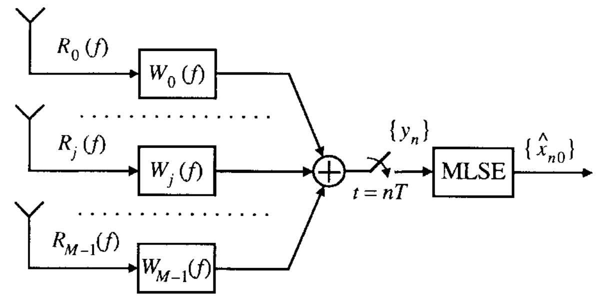

Fig. 2. A space–time MLSE receiver.

distributed complex variables with zero mean and unit symbol energy and are uncorrelated between sources.

The frequency-domain expression of the above received signal is

$$R_j(f) = \sum_{i=0}^{L} X_i(f) H_{ij}(f) + N_j(f) \tag{2}$$

where $R_j(f)$, $X_i(f)$, $H_{ij}(f)$, and $N_j(f)$ are the Fourier transforms of $r_j(t)$, $\{x_{ni}\}$, $h_{ij}(t)$, and $n_j(t)$, respectively. Since the data have unit symbol energy $E[|X_i(f)|]^2 = 1$ for $|f| \le 1/(2T)$ where $E[\cdot]$ denotes expectation. The noise at each antenna has two-sided power spectrum density N_0.

The general space–time receiver using a DFE is shown in Fig. 1 (an LE receiver model can be obtained by setting the feedback filter response to zero). It consists of a linear feed-forward filter, $W_j(f)$, $j = 0, 1, \cdots, M-1$, on each branch, a combiner, symbol-rate sampler, slicer, and synchronous linear feedback filter $B(f)$. The feedforward filters $\{W_j(f)\}$ are shown as continuous-time filters, but they can be implemented in practice using fractionally-spaced tapped delay lines. The input to the feedback filter is the decided data $\{\hat{x}_{n0}\}$ for the desired source. We assume correct decisions ($\hat{x}_{n_0} = x_{n0}$) throughout this study.

The input to the slicer (i.e., the space–time processor output) is denoted by sequence $\{y_n\}$, with its Fourier transform $Y(f)$ given by

$$Y(f) = \sum_{j=0}^{M-1} \sum_{m=-\infty}^{\infty} W_j\Big(f - \frac{m}{T}\Big) R_j\Big(f - \frac{m}{T}\Big) - B(f) X_0(f). \tag{3}$$

The summation with respect to m in the above equation is a result of spectrum folding due to symbol-rate sampling.

Based on the MMSE criterion, the filters are optimized by minimizing the mean square error (MSE)

$$\epsilon = E[|y_n - x_{n0}|^2] = T \int_{-(1/2T)}^{1/2T} E[|Y(f) - X_0(f)|^2]\, df. \tag{4}$$

Fig. 2 shows a space–time receiver using an MLSE. Here, the goal of optimization is to maximize the signal power (without suppressing ISI) to CCI plus noise power ratio, while whitening the CCI and noise components of the input $\{y_n\}$ to the MLSE.

Our analysis also includes the use of z-transforms. The z-transform of a sampled sequence of a continuous-time function $g(t)$ is $\tilde{G}(z) \triangleq \Sigma_k g_k z^{-k}$, where $g_k = T \cdot g(kT)$ [we multiply $g(kT)$ by T so that $\{g_k\}$ and $g(t)$ have the same average energy per symbol interval]. The relation between z-transform and Fourier transform is given by the following using the Poisson sum formula [13]:

$$\tilde{G}(e^{\mathbf{j}2\pi fT}) = \sum_{k=-\infty}^{\infty} g_k e^{-\mathbf{j}2\pi kfT} = \sum_{m=-\infty}^{\infty} G\Big(f - \frac{m}{T}\Big) \tag{5}$$

where $G(f)$ is the Fourier transform of $g(t)$, and $\mathbf{j} = \sqrt{-1}$. It is easy to show that

$$T \int_{-(1/2T)}^{1/2T} G'(f)\, df = \frac{1}{2\pi\mathbf{j}} \oint \tilde{G}(z) \frac{dz}{z} \tag{6}$$

where $G'(f) \triangleq \sum_{m=-\infty}^{\infty} G(f - (m/T))$ is the Fourier transform of the sequence $\{g_k\}$. The contour of the integration on the right side of (6) is the unit circle. For convenience, we omit the tilde sign from our z-transform notation throughout the rest of this paper, e.g., $\tilde{G}(z)$ will be written simply as $G(z)$. Furthermore, if $G(f)$ is the Fourier transform of a symbol-spaced sequence (instead of a continuous-time function), then

$$T \int_{-(1/2T)}^{1/2T} G(f)\, df = \frac{1}{2\pi\mathbf{j}} \oint G(z) \frac{dz}{z}. \tag{7}$$

III. Unified Infinite-Length Theory

A. Optimum Filter Expressions for DFE and LE Receivers

The MMSE solution for the feedforward filters $\{W_j(f)\}$ with unconstrained length can be derived by using (2)–(4) and setting the derivatives $\{\partial\epsilon/\partial W_j(f - (m/T))\}$ to zero. This yields

$$\mathbf{W} = [\mathbf{R}_S + \mathbf{R}_{IN}]^{-1} \mathbf{H}_0^* (1 + B(f)) \tag{8}$$

where

$$\mathbf{W} \triangleq \Big[W_0\Big(f - \frac{J}{T}\Big) \cdots W_{M-1}\Big(f - \frac{J}{T}\Big) \cdots W_0\Big(f + \frac{J}{T}\Big) \cdots W_{M-1}\Big(f + \frac{J}{T}\Big) \Big]^T \tag{9}$$

$$\mathbf{H}_i \triangleq \left[H_{i0}\left(f-\frac{J}{T}\right)\cdots H_{i,M-1}\left(f-\frac{J}{T}\right)\cdots H_{i0}\left(f+\frac{J}{T}\right)\cdots H_{i,M-1}\left(f+\frac{J}{T}\right)\right]^T \tag{10}$$

$$\mathbf{R}_S \triangleq \mathbf{H}_0^*\mathbf{H}_0^T \tag{11}$$

$$\mathbf{R}_{I+N} \triangleq \sum_{i=1}^{L} \mathbf{H}_i^*\mathbf{H}_i^T + N_0\mathbf{I}. \tag{12}$$

$\mathbf{R}_S$ is the correlation matrix of the desired signal, $\mathbf{R}_{I+N}$ is the correlation matrix of the interference plus noise, $\mathbf{I}$ is the identity matrix, and the superscripts $*$ and T denote complex conjugate and transpose, respectively. We assume that the desired and CCI sources are strictly band limited to $f = \pm J'/(2T)$ (J' is a positive integer), and therefore $J=(J'-1)/2$ when J' is odd, and $J=J'/2$ when J' is even (e.g., $J'=1$ and $J=0$ when there is no excess bandwidth). Note in (9) and (10) that excess bandwidth provides additional diversity which can be exploited when there is sufficient transmit power outside the Nyquist band, e.g., in a spread spectrum system [14] (or see also [17]).

Using the matrix inversion lemma [12, Appendix D], it can be shown that

$$[\mathbf{R}_S+\mathbf{R}_{I+N}]^{-1}\mathbf{H}_0^* = \frac{\mathbf{R}_{I+N}^{-1}\mathbf{H}_0^*}{1+\mathbf{H}_0^T\mathbf{R}_{I+N}^{-1}\mathbf{H}_0^*}. \tag{13}$$

Therefore, (8) becomes

$$\mathbf{W} = \frac{\mathbf{R}_{I+N}^{-1}\mathbf{H}_0^*}{1+\mathbf{H}_0^T\mathbf{R}_{I+N}^{-1}\mathbf{H}_0^*}(1+B(f)). \tag{14}$$

Furthermore, we can define the signal-to-interference-plus-noise power density ratio $\Gamma(f)$ at frequency f as

$$\Gamma(f) = \frac{\mathbf{W}^\dagger\mathbf{R}_S\mathbf{W}}{\mathbf{W}^\dagger\mathbf{R}_{I+N}\mathbf{W}} \tag{15}$$

where the superscript $\dagger$ denotes conjugate transpose ($\mathbf{W}^\dagger\mathbf{R}_S\mathbf{W}$ is the output signal power density, and $\mathbf{W}^\dagger\mathbf{R}_{I+N}\mathbf{W}$ is the output interference-plus-noise density at frequency f). Substituting (14) into (15) yields

$$\Gamma(f) = \mathbf{H}_0^T\mathbf{R}_{I+N}^{-1}\mathbf{H}_0^*. \tag{16}$$

Thus, we can rewrite the optimum feedforward filter solution as

$$\mathbf{W} = \mathbf{R}_{I+N}^{-1}\mathbf{H}_0^*\frac{1+B(f)}{1+\Gamma(f)}. \tag{17}$$

Equation (17) gives the form of the MMSE solution, well known in array processing [12] (except for the consideration of spectrum folding and feedback filtering). This equation indicates that the optimum feedforward filter consists of a space–time filter $\mathbf{R}_{I+N}^{-1}\mathbf{H}_0^*$, which performs spatial prewhitening ($\mathbf{R}_{I+N}^{-1/2}$ is the whitening filter of CCI and noise) and matching to the desired channel, followed by a temporal filter $(1+B(f))/(1+\Gamma(f))$, which can be regarded as a post-whitening filter under some zero-forcing condition, as described below.

The optimum feedback filter $B(f)$ can be determined through spectrum factorization. Substituting (17) into (3), and using (4) and (7), we obtain

$$\epsilon = T\int_{-(1/2T)}^{1/2T}\frac{|1+B(f)|^2}{1+\Gamma(f)}\,df \tag{18}$$

$$= \frac{1}{2\pi\mathbf{j}}\oint\frac{(1+B(z))(1+B^*(z^{-1}))}{1+\Gamma(z)}\frac{dz}{z} \tag{19}$$

where $B(z)$ and $\Gamma(z)$ are the z-transform equivalents of $B(f)$ and $\Gamma(f)$. Using spectral factorization theory [19], $1+\Gamma(f)$ and $1+\Gamma(z)$ can be written as

$$1+\Gamma(f) = S_0|G(f)|^2;\quad 1+\Gamma(z) = S_0G(z)G^*(z^{-1}) \tag{20}$$

where the constant S_0 is given by

$$S_0 = e^{\langle\ln(1+\Gamma(f))\rangle} \tag{21}$$

and

$$\langle\cdot\rangle \triangleq T\int_{-(1/2T)}^{1/2T}[\cdot]\,df \tag{22}$$

and $G(z)$ is *canonical*, meaning that it is *causal* ($g_k=0$ for $k<0$), *monic* ($g_0=1$), and *minimum phase* (all of its poles are inside the unit circle, and all of its zeros are on or inside the unit circle).

Using the Schwarz inequality, it can be shown that the MSE in (18) is minimized when

$$1+B(f) = G(f);\quad 1+B(z) = G(z). \tag{23}$$

Substituting (20)–(23) into (17) and (18), we obtain

$$\mathbf{W}_{\mathrm{DFE}} = \mathbf{R}_{I+N}^{-1}\mathbf{H}_0^*\frac{1}{S_0G^*(f)} \tag{24}$$

and

$$\epsilon_{\mathrm{DFE}} = \frac{1}{S_0} = e^{-\langle\ln(1+\Gamma(f))\rangle}. \tag{25}$$

Using (16), (20), and (24), the CCI plus noise power density at frequency f is

$$\mathbf{W}^\dagger\mathbf{R}_{I+N}\mathbf{W} = \frac{\mathbf{H}_0^T\mathbf{R}_{I+N}^{-1}\mathbf{H}_0^*}{S_0^2|G(f)|^2} = \frac{\Gamma(f)}{S_0(1+\Gamma(f))}. \tag{26}$$

Note that as $\Gamma(f)\to\infty$ for $|f|\le 1/(2T)$, the CCI plus noise power density becomes a constant $1/S_0$ over f. Under this condition, we can regard $1/S_0G^*(f)$ in (24) [or $1+B(f)/1+\Gamma(f)$ in (17)] as a post-whitening filter.

As will be relevant later, we can write $1+B(z)$ also as

$$1+B(z) = C[1+\Gamma(z)] \tag{27}$$

where $C[\cdot]$ denotes canonical factor. The corresponding Fourier transform is given as

$$1+B(f) = C[1+\Gamma(f)]. \tag{28}$$

Using the above expression, we can write (17) as

$$\mathbf{W}_{\mathrm{DFE}} = \mathbf{R}_{I+N}^{-1}\mathbf{H}_0^*\frac{C[1+\Gamma(f)]}{1+\Gamma(f)}. \tag{29}$$

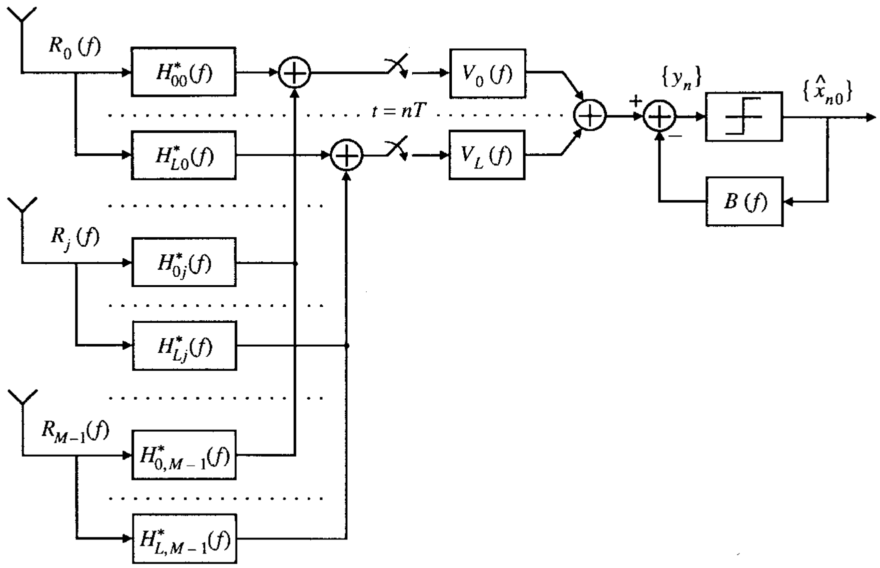

Fig. 3. An equivalent model of the space–time DFE receiver in Fig. 1.

The optimum LE is obtained by setting $B(f)$ to zero in (17) and (18)

$$\mathbf{W}_{\text{LE}} = \mathbf{R}_{I+N}^{-1}\mathbf{H}_0^* \frac{1}{1+\Gamma(f)} \tag{30}$$

and

$$\epsilon_{\text{LE}} = \left\langle \frac{1}{1+\Gamma(f)} \right\rangle. \tag{31}$$

B. An Alternative Solution for DFE and LE Receivers

The optimum space–time filter solution in (17) is based on a general model which does not make any prior assumptions regarding the filter structure. Without loss of optimality, an analytical receiver model suggested by many in the literature (e.g., [15]–[18]) assumes the use of a bank of matched filters $\{H_{ij}^*(f)\}$, each corresponding to the signal source i on diversity branch j, which, after diversity combining, is followed by a bank of T-spaced transversal filters $\{V_i(f)\}$, each corresponding to the signal source i (see Fig. 3). This analytical model leads to a different form of solutions which are important to our filter length analysis. The following derivation is similar to the LE receiver derivation in [18], but here we also provide the solution for the DFE.

In Fig. 3, the Fourier transform of the input to the slicer can be written as

$$Y(f) = \sum_{i=0}^{L} D_i(f)X_i(f) + \aleph(f) - B(f)X_0(f) \tag{32}$$

where $D_0(f)$ and $D_i(f)$ are the overall channel and feedforward filter responses for the desired signal and the ith interference, and $\aleph(f)$ is the noise at the combined output of the feedforward filters. Let $\mathbf{D} = [D_0(f) \ \cdots \ D_L(f)]^T$ and $\mathbf{V} = [V_0(f) \ \cdots \ V_L(f)]^T$. We then have the following relationship:

$$\mathbf{D} = \mathbf{PV} \tag{33}$$

where $\mathbf{P}$ is an $(L+1) \times (L+1)$ correlation matrix whose $(a,\, b)$th element p_{ab} is given by

$$p_{ab} = \sum_{j=0}^{M-1} \sum_{m=-\infty}^{\infty} H_{aj}\Big(f - \frac{m}{T}\Big)H_{bj}^*\Big(f - \frac{m}{T}\Big). \tag{34}$$

Furthermore, we can write

$$D_0(f) = \mathbf{V}^T\mathbf{P}^T\mathbf{U} \tag{35}$$

where $\mathbf{U} = [1,\, 0,\, \cdots,\, 0]^T$ is a column vector with $L+1$ rows, and

$$\sum_{i=0}^{L} |D_i(f)|^2 = \mathbf{V}^\dagger\mathbf{P}^\dagger\mathbf{P}\mathbf{V}. \tag{36}$$

The MSE for this receiver is given by

$$\epsilon = \epsilon_{\text{ISI}} + \epsilon_{\text{CCI}} + \epsilon_{\text{noise}} \tag{37}$$

where

$$\epsilon_{\text{ISI}} = \langle |D_0(f) - (1 + B(f))^2 \rangle \tag{38}$$

$$\epsilon_{\text{CCI}} = \left\langle \sum_{i=1}^{L} |D_i(f)|^2 \right\rangle \tag{39}$$

and

$$\epsilon_{\text{noise}} = \langle N_0\mathbf{V}^\dagger\mathbf{P}\mathbf{V}\rangle = \langle N_0\mathbf{V}^\dagger\mathbf{P}^\dagger\mathbf{V}\rangle. \tag{40}$$

Using (35) and (36), the MSE becomes

$$\begin{aligned}\epsilon = \langle &\mathbf{V}^\dagger\mathbf{P}^\dagger\mathbf{P}\mathbf{V} + N_0\mathbf{V}^\dagger\mathbf{P}^\dagger\mathbf{V} + |1 + B(f)|^2 \\ &- 2\,\text{Re}[(1 + B^*(f))\mathbf{V}^T\mathbf{P}^T\mathbf{U}]\rangle.\end{aligned} \tag{41}$$

The MMSE solution for $\mathbf{V}$ is obtained by solving $(\partial\epsilon/\partial V_i(f)) = 0$ for $i = 0$ to L. We then obtain

$$\mathbf{V} = (\mathbf{P} + N_0\mathbf{I})^{-1}\mathbf{U}(1 + B(f)). \tag{42}$$

It can be shown that this receiver achieves the same MMSE as (25) (or (31) in the case of an LE receiver) and that

$$1 + \Gamma(f) = \frac{1}{N_0} \frac{1}{\mathbf{U}^T(\mathbf{P} + N_0\mathbf{I})^{-1}\mathbf{U}}. \tag{43}$$

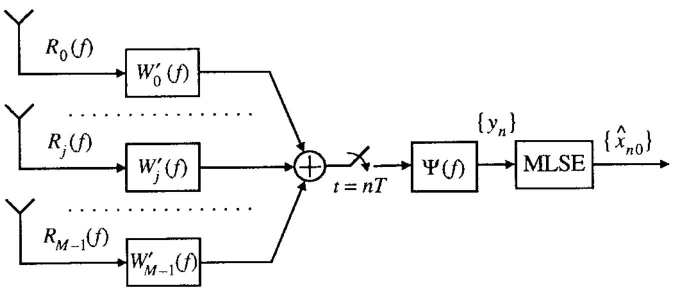

Fig. 4. An equivalent model of the space–time MLSE receiver in Fig. 2.

Again, $1 + B(z)$ is the canonical factor of $1 + \Gamma(z)$. Accordingly, we can rewrite (42) as

$$V_{\mathrm{DFE}} = (\mathbf{P} + N_0\mathbf{I})^{-1}\mathbf{U}C[1 + \Gamma(f)]. \tag{44}$$

For an LE receiver

$$\mathbf{V}_{\mathrm{LE}} = (\mathbf{P} + N_0\mathbf{I})^{-1}\mathbf{U}. \tag{45}$$

C. Optimum Linear Filtering for MLSE

Fig. 4 shows an equivalent model of the MLSE receiver in Fig. 2. The front-end filters are now represented by spatial filters $\{W'_j(f)\}$, which maximize SINR of their combined output, followed by a post-whitening filter $\boldsymbol{\Psi}(f)$. Let $\mathbf{W}'$ denote the vector of $\{W'_j(f)\}$ similar to (9). The signal-to-interference-plus-noise power density ratio $\Gamma(f)$ is then [cf. (15)]

$$\Gamma(f) = \frac{\mathbf{W}'^{\dagger}\mathbf{R}_S\mathbf{W}'}{\mathbf{W}'^{\dagger}\mathbf{R}_{I+N}\mathbf{W}'}. \tag{46}$$

The optimum $\mathbf{W}'$ is obtained by solving $(\partial\Gamma(f)/\partial W'_j(f)) = 0$, for $j = 0, 1, \cdots, M-1$; this gives the relationship

$$\mathbf{R}_S\mathbf{W}' = \Gamma(f)\mathbf{R}_{I+N}\mathbf{W}'. \tag{47}$$

The maximum $\Gamma(f)$ is, therefore, given by the maximum eigenvalue of $\mathbf{R}_{I+N}^{-1}\mathbf{R}_S$. Let $\mathbf{W}'_{\mathrm{opt}}$ be the eigenvector corresponding to this maximum eigenvalue, and substitute $\mathbf{W}' = \mathbf{W}'_{\mathrm{opt}}$ into (46). We obtain

$$\mathbf{W}'_{\mathrm{opt}} = \beta(f)\mathbf{R}_{I+N}^{-1}\mathbf{H}_0^* \tag{48}$$

where

$$\beta(f) = \frac{\mathbf{W}'_{\mathrm{opt}}\mathbf{R}_{I+N}\mathbf{W}'_{\mathrm{opt}}}{\mathbf{W}'_{\mathrm{opt}}\mathbf{H}_0^*}. \tag{49}$$

Equation (48) has the same form as (17). As a result, we obtain the same expression for $\Gamma(f)$ as (16). By factoring $\Gamma(f)$ as

$$\Gamma(f) = S_1|C[\Gamma(f)]|^2 \tag{50}$$

we can find a post-whitening filter

$$\Psi(f) = \frac{C[\Gamma(f)]}{\beta(f)\Gamma(f)} \tag{51}$$

which satisfies

$$\begin{aligned}\mathbf{W}^{\dagger}\mathbf{R}_{I+N}\mathbf{W} &= |\beta(f)|^2|\Psi(f)|^2\mathbf{H}_0^T\mathbf{R}_{I+N}^{-1}\mathbf{H}_0^* \\ &= \frac{|C[\Gamma(f)]|^2\Gamma(f)}{|\Gamma(f)|^2} \\ &= \frac{1}{S_1} \\ &= \text{constant}\end{aligned} \tag{52}$$

where the overall filter response $\mathbf{W}$ is given by

$$\mathbf{W} = \mathbf{W}'\Psi(f) = \mathbf{R}_{I+N}^{-1}\mathbf{H}_0^*\,\frac{C[\Gamma(f)]}{\Gamma(f)}. \tag{53}$$

Comparing (53) to (29), we find that

$$\mathbf{W}_{\mathrm{MLSE}} = \mathbf{W}_{\mathrm{DFE}} \cdot \frac{1 + \Gamma(f)}{C[1 + \Gamma(f)]} \cdot \frac{C[\Gamma(f)]}{\Gamma(f)}. \tag{54}$$

This relationship is extendable to the case where we use the analytical feedforward filter model in Fig. 3 to represent the front-end filter of the MLSE receiver. Thus, we can also write

$$\mathbf{V}_{\mathrm{MLSE}} = \mathbf{V}_{\mathrm{DFE}} \cdot \frac{1 + \Gamma(f)}{C[1 + \Gamma(f)]} \cdot \frac{C[\Gamma(f)]}{\Gamma(f)}. \tag{55}$$

Accordingly

$$\mathbf{V}_{\mathrm{VLSE}} = (\mathbf{P} + N_0\mathbf{I})^{-1}\mathbf{U}(1 + \Gamma(f))\,\frac{C[\Gamma(f)]}{\Gamma(f)}. \tag{56}$$

In (54), when $\Gamma(f) \gg 1$ such that $1 + \Gamma(f) \approx \Gamma(f)$, then $\mathbf{W}_{\mathrm{MLSE}} \approx \mathbf{W}_{\mathrm{DFE}}$, i.e., the optimum front-end filter for an MLSE receiver is equivalent to the optimum feedforward filter of a DFE receiver. This is usually the case when there is no CCI and the input SNR is sufficiently high [20]. However, it is generally not true in the presence of strong CCI's.

Also, using (53) and (56), it can be shown that

$$\mathbf{H}_0^T\mathbf{W} = D_0(f) = C[\Gamma(f)]. \tag{57}$$

Thus, the desired signal at the output of the front-end filter has a canonical impulse response; this is the known desired property of the input to an MLSE [21] (in addition to the noise being white).

IV. Filter Length Analysis

Our filter length analysis is based on counting the number of zeros and poles in the z-transform expression of the optimum space–time filter. For all three receivers (LE, DFE, and MLSE), there are two forms of optimum filter solutions:

1) one based on the general model (with a linear filter on each branch);
2) one based on the analytical model (with a bank of matched filters on each branch, followed by common filters).

The filter length determined by each solution is valid under different assumptions. The filter length based on the general model is valid when $M < L+1$, i.e., when the number of interferers is equal to or greater than the order of diversity due to multiple antennas and excess bandwidth for convenience, we write the overall order of diversity as M, instead of M_j'. The filter length based on the analytical model is valid when $M \geq L+1$. The reason for these different conditions will become apparent later.

Since the general analytical approach for determining the filter length is the same for both solution forms, we only provide details for one of them below. We choose to work on the analytical model case because it is slightly more complicated than the other case, and because the condition under which it is valid (the order of diversity exceeding the number of dominant interferers) is where the most interference suppression is achieved, i.e., an array with M antennas can null up to $M-1$ interferers [23].

We begin by working on the MMSE solution for the DFE receiver. The z-transform equivalent of (42) is

$$\begin{aligned}\mathbf{V} &= (\mathbf{P}+N_0\mathbf{I})^{-1}\mathbf{U}(1+B(z))\\ &\triangleq \mathbf{Q}^{-1}\mathbf{U}(1+B(z))\end{aligned} \tag{58}$$

where $\mathbf{V} \triangleq [V_0(z) \ \cdots \ V_L(z)]^T$ and $\mathbf{Q} \triangleq \mathbf{P}+N_0\mathbf{I}$. The element p_{ab} of matrix $\mathbf{P}$ is the z-transform of the sampled sequence of

$$\sum_{j=0}^{M-1}\int_{-\infty}^{\infty} h_{aj}(\tau)h_{bj}^*(\tau-t)\,d\tau. \tag{59}$$

Thus, each element q_{ab} of matrix $\mathbf{Q}$ has a two-sided response such that it includes both a causal factor and an anticausal factor of equal length. If we assume that all channels $\{h_{ij}(t)\}$ have a finite memory of K symbol periods ($h_{ij}(t)=0$ for $t<0$ and $t>KT$), then the causal and anticausal factors of q_{ab} will be polynomials of order K.

Using the matrix identity [22]

$$\mathbf{Q}^{-1} = \frac{\mathbf{Q}_{\text{adj}}}{|\mathbf{Q}|} \tag{60}$$

where $\mathbf{Q}_{\text{adj}}$ is called the *adjugate matrix* of matrix $\mathbf{Q}$, and the (a, b)th element Q_{ab} of the transpose matrix of $\mathbf{Q}_{\text{adj}}$ is called the *cofactor* corresponding to the (a, b)th element q_{ab} of matrix $\mathbf{Q}$ [$Q_{ab} = (-1)^{a+b}|\overline{\mathbf{Q}}_{ab}|$, where $\overline{\mathbf{Q}}_{ab}$ is obtained by deleting the ath row and bth column of $\mathbf{Q}$], we can rewrite (58) as

$$\begin{aligned}\mathbf{V} &= \frac{\mathbf{Q}_{\text{adj}}}{|\mathbf{Q}|}\mathbf{U}(1+B(z))\\ &= \frac{[Q_{00} \quad Q_{01} \quad \cdots \quad Q_{0L}]^T}{|\mathbf{Q}|}(1+B(z))\end{aligned} \tag{61}$$

where $1+B(z)$ is given by [see (43)]

$$\begin{aligned}1+B(z) &= C[1+\Gamma(z)]\\ &= C\left[\frac{1}{N_0\mathbf{U}^T\mathbf{Q}^{-1}\mathbf{U}}\right]\\ &= \frac{C[|\mathbf{Q}|]}{C[Q_{00}]}.\end{aligned} \tag{62}$$

Thus, we obtain

$$\mathbf{V} = \frac{[Q_{00} \quad Q_{01} \quad \cdots \quad Q_{0L}]^T}{(|\mathbf{Q}|/C[|\mathbf{Q}|])\cdot C[Q_{00}]}. \tag{63}$$

Note that the common filter for the desired signal is

$$V_0(z) = \frac{Q_{00}/C[Q_{00}]}{|\mathbf{Q}|/C[|\mathbf{Q}|]}. \tag{64}$$

Thus, this filter is anticausal (cf. [17]).

We now focus on each term in (63). Defining a permutation σ as a one-to-one mapping σ: $(0, 1, \cdots, L) \rightarrow (\sigma_0, \sigma_1, \cdots, \sigma_L)$, the determinant of $\mathbf{Q}$ is [22]

$$|\mathbf{Q}| = \sum_{\sigma}\text{sgn}(\sigma)q_{0\sigma_0} \quad q_{1\sigma_1} \quad \cdots \quad q_{L\sigma_L} \tag{65}$$

where $\text{sgn}(\sigma) = +1$ or -1 depending on whether the number of exchanges in permutation σ is even or odd, and the summation is taken over all $(L+1)!$ permutations σ. Note that the product of two polynomials of order a and b results in a polynomial of order $a+b$, while the sum of them gives a polynomial of order $\max[a, b]$. Since each element q_{ab} of matrix $\mathbf{Q}$ includes a causal factor and an anticausal factor, each of order K, $|\mathbf{Q}|$ will, in general, have a causal factor and anticausal factor, each of order $K(L+1)$. Similarly, Q_{ab} will, in general, have a causal factor and anticausal factor, each of order KL. Accordingly, $|\mathbf{Q}|/C[|\mathbf{Q}|]$ will be anticausal (and maximum phase) with order $K(L+1)$, and $C[Q_{00}]$ will be causal (and minimum phase) with order KL. Combining these results together, the causal part of each filter $V_i(z)$ (for $i>0$) will have KL zeros and KL poles, and its anticausal part will have KL zeros and $K(L+1)$ poles. Since each front-end matched filter $h_{ij}^*(-t)$ is anticausal with length K (we can always set the synchronization timing such that $h_{ij}(t)$ is a causal function), the overall feedforward filter on each branch will have a causal part with KL zeros and KL poles and an anticausal part with $K(L+1)$ zero and $K(L+1)$ poles.

In general, a pole filter has an infinite impulse response. Nevertheless, we can always truncate a pole filter which is causal and minimum phase, or anticausal and maximum phase, such that the effect of truncation is small compared to the background noise. Thus, the lengths in units of T of the causal and anticausal parts (denoted as C and A, respectively) of the optimum feedforward filter can be given as

$$\begin{aligned}&\text{DFE } (M \geq L+1){:} \quad C = KL(1+\alpha)\\ &\qquad A = K(L+1)(1+\alpha).\end{aligned} \tag{66}$$

Here, α determines the truncated length of a pole filter $(1-\xi z)^{-1}$ or $(1-\xi z^{-1})^{-1}$. Note that $C=0$ when $L=0$; this agrees with the known result that, in the absence of CCI, the optimum feedforward filter of a DFE is anticausal.

Note that the required length of the feedback filter is $K+C$, since the optimum feedback filter completely cancels the postcursors of the desired signal.

Similarly, we can estimate the filter length for an LE receiver using (61), with $B(z)$ set to zero; this gives

$$\begin{aligned}&\text{LE } (M \geq L+1):\\ &\quad C = K(L+1)(1+\alpha) - K\\ &\quad A = K(L+1)(1+\alpha).\end{aligned} \tag{67}$$

Note that the causal length of the LE receiver is greater (by $K\alpha$) than that of the feedforward filter of the DFE receiver.

The above results are valid under the condition that the MMSE solution in (61) is *compact*, meaning that there is no cancellation of highest order terms in the summation in (65) for all determinants. By working on specific examples, we found (61) to be compact when $M \geq L+1$. Otherwise, the MMSE solution based on the general filter model [given in (17)] is compact.

Using the same analytical approach as above, we estimate the filter length for the case $M < L+1$ as

$$\begin{aligned}&\text{LE and DFE } (M < L+1):\\ &\quad C = KM(1+\alpha) - K\\ &\quad A = KM(1+\alpha).\end{aligned} \tag{68}$$

The filter length results are the same for both LE and DFE receivers in this case.

We now focus on the MLSE receiver. Using (63) and the relationship in (55), we obtain

$$\mathbf{V}_{\text{MLSE}} = \frac{[Q_{00} \quad Q_{01} \quad \cdots \quad Q_{0L}]^T}{((|\mathbf{Q}| - N_0 Q_{00})/C[|\mathbf{Q}| - N_0 Q_{00}]) \cdot C[Q_{00}]}. \tag{69}$$

Comparing (69) with (63), we see that individual terms in the two equations have the same highest order and, thus, the two filters have the same length. This is also true when we compare the filter lengths using the general filter model. We, therefore, conclude that the optimum front-end filter for the MLSE receiver has the same length as the optimum feedforward filter of the DFE receiver; namely

$$\begin{aligned}&\text{MLSE } (M \geq L+1):\\ &\quad C = KL(1+\alpha)\\ &\quad A = K(L+1)(1+\alpha)\end{aligned} \tag{70}$$

and

$$\begin{aligned}&\text{MLSE } (M < L+1):\\ &\quad C = KM(1+\alpha) - K\\ &\quad A = KM(1+\alpha).\end{aligned} \tag{71}$$

Note that the above analysis does not take into account the effect of thermal noise, i.e., strictly speaking, the filter length expressions given above are valid only when the input SNR approaches infinity. As the SNR decreases, we expect the required length of the whitening filter $\mathbf{V}$ or $\mathbf{R}_{I+N}^{-1}S(z)$ ($S(z)$ denotes the temporal filter, e.g., $S(z) = 1/(1+\Gamma(z))$ for an LE receiver) to decrease and eventually approach zero when thermal noise dominates both CCI and ISI. Although analytical results are not available, it is possible to study this effect through numerical examples, as shown in the next section. Nevertheless, the general relationship regarding how the required length of the whitening filter varies with the dispersion length, number of interferers, and order of diversity, should remain unchanged for any given SNR.

V. Numerical Results

We now study the effect of thermal noise on the required filter span of DFE and LE receivers. As discussed earlier, we expect the required filter span of an MLSE receiver to be the same as that of a DFE receiver (although this needs to be proven for all given SNR's). For the purpose of illustration, we assume a single-carrier system using quaternary phase-shift keying with Nyquist filtering. We also assume a *multiray* delay profile for all the channels, where all the rays are of equal power, independently Rayleigh faded, and uniformly spaced by an interval T (the symbol period). The fading is assumed to be independent for different signal sources and diversity branches. We choose this channel model for several reasons: first, we define the rays to be T-spaced so that, with Nyquist filtering, the channel memory is strictly restricted to K, for a given $K+1$-ray delay profile (see the discussion at the end of this section regarding cases where the channel memory is not strictly restricted to K). Furthermore, since the frequency response of a T-spaced multiray channel is periodic, with period $1/T$, there is no need to consider spectrum folding in our numerical computations. Accordingly, we assume the use of T-spaced equalizers in all the finite-length performance results. Finally, we assume the rays to be equal power so that the results obtained give a worst case (i.e., more conservative) estimate of the required filter length for a given channel memory compared to channel models with unequal delayed paths.

Fig. 5(a)–(c) show the infinite-length performance of MMSE-DFE and MMSE-LE receivers compared to the matched filter (MF) bound. The performance is given in terms of the average bit error rate (BER) as a function of the average input SNR, where the average is over Rayleigh fading. The fading of individual channels was generated by Monte Carlo simulation. For a given set of channel realizations, the BER was computed as

$$P_b = \frac{1}{2}\,\text{erfc}\left(\sqrt{\frac{\gamma_o}{2}}\right) \tag{72}$$

where $\text{erfc}(\cdot)$ is the complementary error function [13], and the output SNR γ_o is given by [19]

$$\gamma_o = \frac{1}{\epsilon_{\text{DFE}}} - 1, \qquad \text{for DFE} \tag{73}$$

$$\gamma_o = \frac{1}{\epsilon_{\text{LE}}} - 1, \qquad \text{for LE} \tag{74}$$

and

$$\gamma_o = \langle \Gamma(f) \rangle \tag{75}$$

and ϵ_{DFE}, ϵ_{LE}, and $\Gamma(f)$ are given by (25), (31), and (16), respectively.

Note that we only consider the case of $M \geq L+1$, i.e., the receiver has a sufficient number of antennas to suppress all

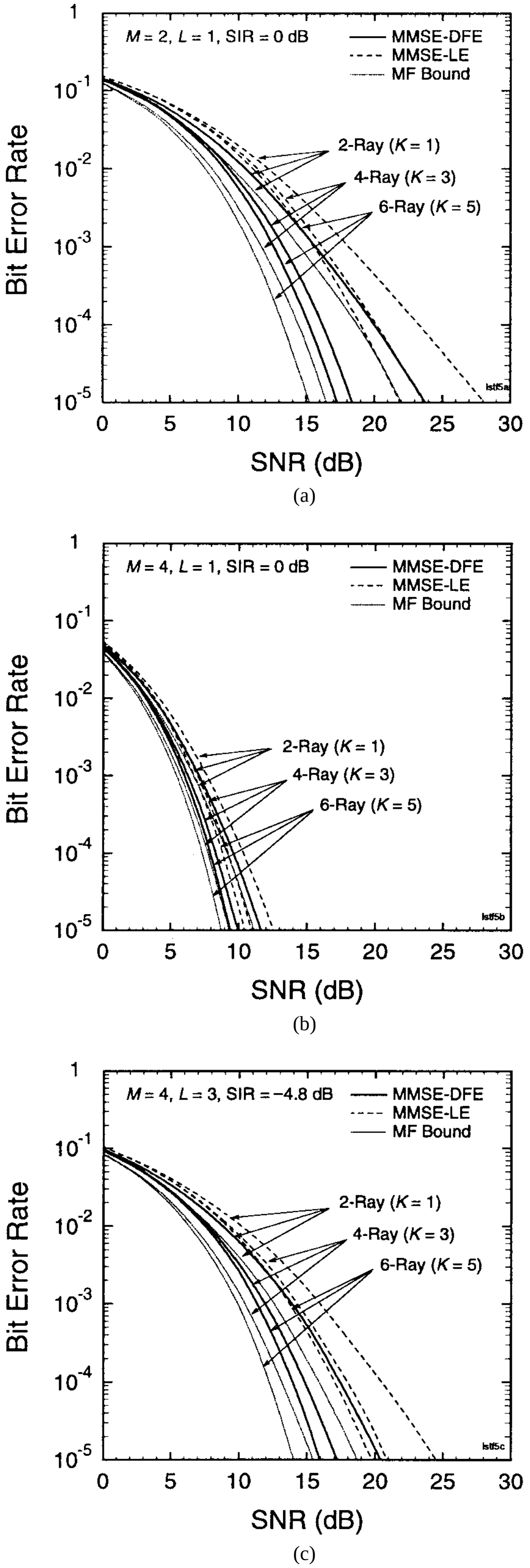

Fig. 5. Infinite-length performance of space–time MMSE-DFE and MMSE-LE, compared to the MF bound. (a) $L = 1, M = 2$. (b) $L = 1, M = 4$. (c) $L = 3, M = 4$.

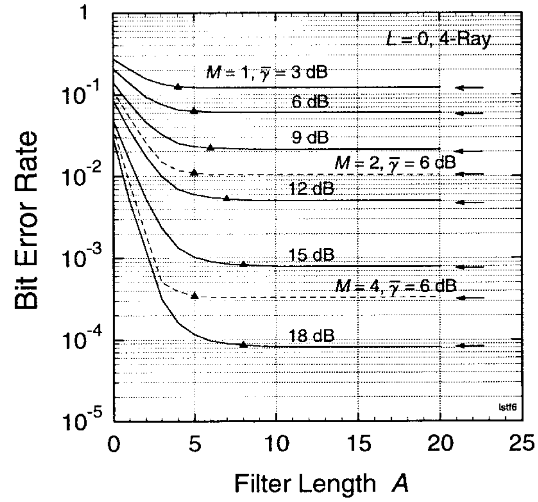

Fig. 6. Effect of SNR on the required filter length of a space–time MMSE-DFE. $L = 0$. Four-ray channel ($K = 3$).

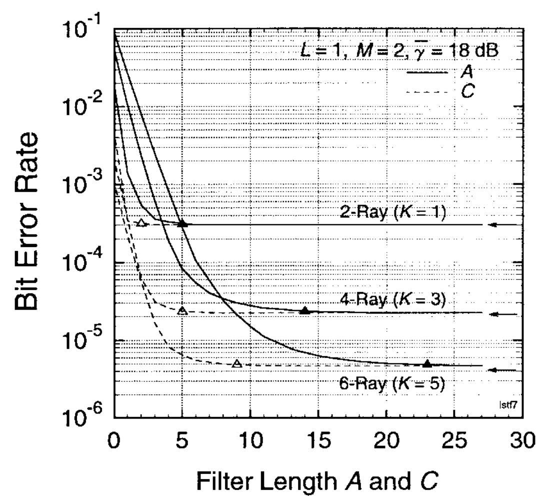

Fig. 7. Effect of channel dispersion length K on the required filter length of a space–time MMSE-DFE. $L = 1$, $M = 2$, and $\overline{\gamma} = 18$ dB.

dominant interferers (the remaining interference can be treated as Gaussian noise if its total energy is sufficiently low). We assume that each of the L interferers has the same power as the desired signal. Thus, the average signal-to-interference ratio is 0 dB for $L = 1$ and -4.8 dB for $L = 3$. Fig. 5(a)–(c) show that the infinite-length DFE performs to within 1–2 dB of the MF bound in all cases, while for $M = L + 1$ [Fig. 5(a) and (c)], the performance of the infinite-length LE is worse than that the MF bound by up to 6 dB, at BER around 10^{-4}.

Fig. 6–9 provide results for finite-length MMSE-DFE and MMSE-LE receivers. In all of these figures, we plot the average BER as a function of the length (the number of symbol-spaced taps) of the causal and/or anticausal portion of the filter on each diversity branch. The total filter length is $C + A + 1$, where C and A are the length of the causal and anticausal portions, respectively, as defined earlier. In all of the figures, the BER is shown to decrease with the filter length until it reaches an asymptotic value (a "floor"). The arrows on the right side of each curve show the corresponding infinite-length BER (due to an artifact of the computation, the infinite-length BER's do not necessarily match the BER floors exactly). The triangle symbol on each curve indicates the required filter

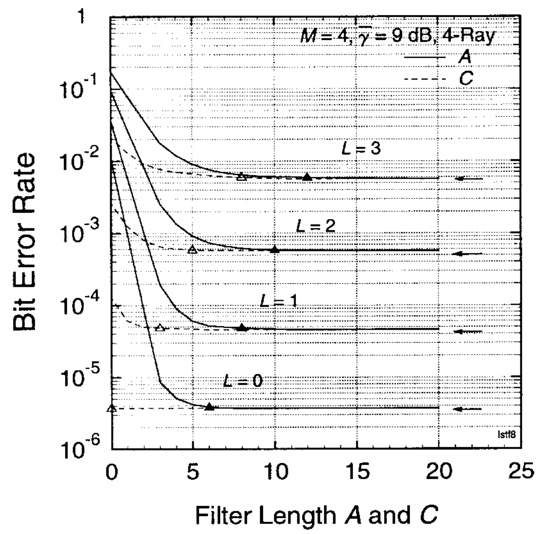

Fig. 8. Effect of the number of interferers L on the required filter length of a space–time MMSE-DFE. $M = 4$, $K = 3$, and $\overline{\gamma} = 9$ dB.

length to achieve "near-optimum" performance, where "near-optimum" is defined here as being within 5% of the BER floor. We assume in all the DFE results (Figs. 6–8) that the feedback filter is sufficiently long such that it completely cancels the postcursor ISI of the desired signal.

Fig. 6 shows the effect of the average input SNR $\overline{\gamma}$ on the required filter length of the DFE receiver, assuming a four-ray channel model $(K = 3)$ with no CCI $(L = 0)$. In this case, the optimum feedforward filter is anticausal [see (66)], so the performance is given only as a function of A. The results for $M = 1$ show that the required filter length to achieve near-optimum performance increases by one for every 3-dB increase in SNR in most cases (the required length stays unchanged when increases from 15 to 18 dB). We will discuss this relationship in more detail later. The example results for $M = 2$ and $M = 4$ show that the required filter length does not change with the number of diversity antennas.

Fig. 7 shows results with different dispersion lengths, assuming $L = 1, M = 2$, and $\overline{\gamma} = 18$ dB. In this case, the performance is given as a function of the lengths of both the causal and anticausal portions of the filter; the results for each portion are obtained by assuming a sufficient length for the other portion. These results show an approximately proportional relationship between the required filter length and the channel dispersion length:

$$\begin{aligned} C &\approx 1.8K \\ A &\approx 4.6K, \qquad \text{for } L = 1, M = 2 \text{ and } \overline{\gamma} = 18 \text{ dB}. \end{aligned} \tag{76}$$

Fig. 8 shows results for different values of L, assuming a four-ray channel model $(K = 3)$ with $M = 4$ and $\overline{\gamma} = 9$ dB. The average SIR is 0, -3, and -4.8 dB for $L = 1$, $L = 2$, and $L = 3$, respectively. The results show that the required filter length grows linearly with the number of interferers.

So far, all the simulation results generally agree with the analytical results in (66), i.e., the required filter length to achieve near-optimum performance grows linearly with K and L, but it does not depend on M. In addition, we found

TABLE I
REQUIRED FILTER LENGTH RESULTS IN FIG. 6, COMPARED WITH PREDICTED LENGTHS BASED ON (77) (SHOWN IN PARENTHESES). $L = 0$, $M = 1$, AND $K = 3$

$\overline{\gamma}$ in dB	3	6	9	12	15	18
A	4 (3.9)	5 (4.8)	6 (5.7)	7 (6.6)	8 (7.5)	8 (8.4)

TABLE II
REQUIRED FILTER LENGTH RESULTS IN FIG. 7, COMPARED WITH PREDICTED LENGTHS BASED ON (77) (SHOWN IN PARENTHESES). $L = 1$, $M = 2$, AND $\overline{\gamma} = 18$ dB

	$K = 1$	$K = 3$	$K = 5$
C	2 (1.8)	5 (5.4)	9 (9)
A	5 (4.6)	14 (13.8)	23 (23)

TABLE III
REQUIRED FILTER LENGTH RESULTS IN FIG. 8, COMPARED WITH PREDICTED LENGTHS BASED ON (77) (SHOWN IN PARENTHESES). $M = 4$, $K = 3$, AND $\overline{\gamma} = 9$ dB

	$L = 0$	$L = 1$	$L = 2$	$L = 3$
C	0 (0)	3 (2.7)	5 (5.4)	8 (8.1)
A	6 (5.7)	8 (8.4)	10 (11.1)	12 (13.8)

in this section that the required filter length grows almost linearly with the average input SNR in decibels. Combining these results together, and taking into account the fact that the anticausal part of the filter always includes a matched filter of length K, we obtain the following empirical formulae for the required filter length:

$$\begin{aligned} \text{DFE:} \quad & C \approx KL\phi(\overline{\gamma}) \\ & A \approx K + K(L+1)\phi(\overline{\gamma}) \end{aligned} \tag{77}$$

where

$$\phi(\overline{\gamma}) = \frac{\overline{\gamma}}{10} \tag{78}$$

and $\overline{\gamma}$ is in decibels. The good agreement between the filter lengths predicted by (77) and the simulation results are shown in Tables I–III. Although not shown here, we also found good agreement when testing the empirical formulae against simulation results with other sets of parameter values.

Despite its empirical nature, (77) has meaningful analytical justifications. First, it gives the same form of expression for C as the analytical result in (66), except for the dependence on the SNR [which is also expected of α in (66)]. Second, when $\overline{\gamma} \to \infty$ such that $\phi(\overline{\gamma}) \gg 1$, the expression for A in (77) becomes $A \to K(L+1)\phi(\overline{\gamma})$; thus, we also obtain the same form of expression for A as (66). As discussed earlier, (66) is also valid when $\overline{\gamma} \to \infty$. Finally, (77) gives the length A as

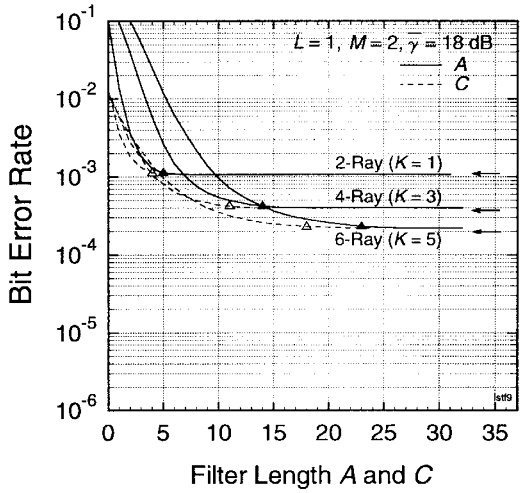

Fig. 9. Required filter length for space–time MMSE-LE. $L = 1$, $M = 2$, and $\overline{\gamma} = 18$ dB.

the sum of the matched filter length K and the length of the anticausal portion of the whitening filter $K(L+1)\phi(\overline{\gamma})$ which decreases with decreasing input SNR; this agrees with the intuition that the length of the whitening filter should approach zero when thermal noise dominates both CCI and ISI.

As for the LE receiver, the analytical results in (67) show that it has the same anticausal length A as that of the DFE receiver, and its causal length is given by $C = A - K$. Thus, we simply modify (77) as

$$\text{LE:}\quad \begin{aligned} C &= K(L+1)\phi(\overline{\gamma}) \\ A &= K + K(L+1)\phi(\overline{\gamma}). \end{aligned} \tag{79}$$

The required filter length results in Fig. 9 agree well with the lengths predicted by the above empirical expressions.

Equations (77) and (79) give useful empirical expressions for predicting the required filter span of space–time DFE and LE receivers for a given SNR. The empirical function $\phi(\overline{\gamma})$ is given in (78) only for a specific channel model (Rayleigh fading and a uniform delay spread profile). This function can be easily determined for other channel environments, by studying only the single-antenna, no CCI performance, similar to the way we determined $\phi(\overline{\gamma})$ from the results in Fig. 6 and Table I.

Note that even if the channel memory is not strictly limited to K, in practice we can truncate the memory such that the energy outside the truncation length is below some given value. The above empirical approach should still be valid in that case as long as K is defined consistently throughout, because $K\phi(\overline{\gamma})$ should be independent of the definition of K. Finally, note that K is typically defined by the system specifications. Our uniform delay profile results give the required filter length for a given K that will meet the system requirements for any delay profile.

VI. Conclusion

In this paper, we studied optimum space–time equalization of dispersive fading channels with CCI. We first presented a unified analysis of optimum space–time equalizers, consisting of a linear filter on each antenna branch, followed by a DFE or MLSE. In this analysis, we derived explicit expressions for the linear filter [e.g., (29), (44), and (54)], which are novel to the best of our knowledge. Using z-transform analysis, we also derived expressions for the linear filter length showing that the required span is proportional to the channel dispersion length and the number of interferers. We then used computer simulation to derive empirical expressions for the required filter span which show that the span is also proportional to the input SNR in decibels. The derived empirical expressions for the required span are in good agreement with simulation results with Rayleigh fading and a uniform-delay spread profile. These expressions are useful in the design of practical near-optimum space–time equalizers.

Acknowledgment

The authors would like to thank M. V. Clark, D. D. Falconer, Y. Li, and L. J. Greenstein for useful discussions and suggestions.

References

[1] A. J. Paulraj and C. B. Papadias, "Space–time processing for wireless communications," *IEEE Signal Processing Mag.*, vol. 14, pp. 49–83, Nov. 1997.
[2] P. Balaban and J. Salz, "Optimum diversity combining and equalization in digital data transmission with applications to cellular mobile radio," *IEEE Trans. Veh. Technol.*, vol. 40, pp. 342–354, May 1991.
[3] J. Salz, "Digital transmission over cross-coupled linear channels," *AT&T Tech. J.*, vol. 64, no. 6, pp. 1147–1159, July/Aug. 1985.
[4] Y. Kim and S. Shamsunder, "Multichannel algorithms for simultaneous equalization and interference suppression," *Wireless Personal Commun.*, vol. 8, no. 2, pp. 219–237, Sept. 1998.
[5] L. Vandendorpe, L. Cuvelier, J. Louveaux, and B. Maison, "Asymptotic performance of MMSE MIMO decision-feedback equalization for uncoded single carrier and multicarrier modulations," in *Proc. IEEE ICC*, Atlanta, GA, 1998, pp. 6–10.
[6] Y. K. Lee and J. J. Shynk, "Separation and equalization of cochannel GSM signals," in *Asilomar Conf. Signals, Systems & Computers*, Pacific Grove, CA, Nov. 1997, presented.
[7] J.-W. Liang, J.-T. Chen, and A. J. Paulraj, "Space–time-filtered Viterbi receiver for CCI/ISI reduction in TDMA systems," in *Circuits Syst. Signal Processing*, 1998, vol. 17, no. 1, pp. 85–102.
[8] T. A. Thomas and M. D. Zoltowski, "Nonparametric interference cancellation and equalization for narrowband TDMA communications via space–time processing," in *IEEE Signal Processing Workshop on Signal Processing Advances in Wireless Communications (SPAWC'97)*, Paris, France, Apr. 1997, pp. 185–188.
[9] D. T. M. Slock, "Spatio-temporal training-sequence-based channel equalization and adaptive interference cancellation," in *Proc. IEEE Int. Conf. Acoustics, Speech, and Signal Processing (ICASSP'96)*, Atlanta, GA, May 1996, pp. 2714–2717.
[10] K. J. Molnar and G. E. Bottomley, "D-AMPS performance in PCS bands with array processing," in *Proc. IEEE Vehicular Technology Conf. (VTC'96)*, Atlanta, GA, Apr./May 1996, pp. 1496–1500.
[11] G. G. Raleigh and A. J. Paulraj, "Time varying vector channel estimation for adaptive spatial equalization," in *Proc. IEEE GLOBECOM'95*, Singapore, Nov. 1995, pp. 218–224.
[12] R. A. Monzingo and T. W. Miller, *Introduction to Adaptive Arrays*. New York: Wiley, 1980.
[13] J. G. Proakis, *Digital Communications*, 2nd Ed. New York: McGraw-Hill, 1989.
[14] M. K. Simon, J. K. Omura, R. A. Scholtz, and B. K. Levitt, *Spread Spectrum Communications*. Rockville, MD: Computer Science, 1985.
[15] A. R. Kaye and D. A. George, "Transmission of multiplexed PAM signals over multiple channel and diversity systems," *IEEE Trans. Commun. Technol.*, vol. COM-18, pp. 520–526, Oct. 1970.
[16] W. Van Etten, "An optimum linear receiver for multiple channel digital transmission systems," *IEEE Trans. Commun.*, Aug. 1975, pp. 828–834.
[17] B. R. Petersen and D. D. Falconer, "Minimum mean square equalization in cyclostationary and stationary interference: Analysis and subscriber

line calculations," *IEEE J. Select. Areas Commun.*, vol. 9, pp. 931–940, Aug. 1991.
[18] M. V. Clark, L. J. Greenstein, W. K. Kennedy, and M. Shafi, "Optimum linear diversity receivers for mobile communications," *IEEE Trans. Veh. Technol.*, vol. 43, pp. 47-56, Feb. 1994.
[19] J. M. Cioffi, G. P. Dudevoir, M. V. Eyuboglu, and G. D. Forney, Jr., "MMSE decision-feedback equalizers and coding—Part I: Equalization results," *IEEE Trans. Commun.*, vol. 43, pp. 2582–2594, Oct. 1995.
[20] D. G. Messerschmitt, "Design of a finite impulse response for the Viterbi algorithm and decision-feedback equalizer," in *Proc. IEEE ICC'74*, Minneapolis, MN, June 1974, pp. 37D-1–37D-5.
[21] G. D. Forney, Jr., "Maximum-likelihood sequence estimation of digital sequence in the presence of intersymbol interference," *IEEE Trans. Inform. Theory*, vol. IT-18, pp. 363–378, May 1972.
[22] G. Strang, *Linear Algebra and Its Applications*. Orlando, FL: Harcourt Brace Jovanovich, 1980.
[23] J. H. Winters, J. Salz, and R. D. Gitlin, "The impact of antenna diversity on the capacity of wireless communications systems," *IEEE Trans. Commun.*, vol. 42, pp. 1740–1751, Apr. 1994.

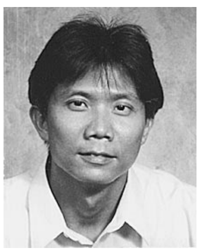

Sirikiat Lek Ariyavistakul (S'85–M'88–SM'93) received the B.S., M.S., and Ph.D. degrees in electrical engineering from Kyoto University, Kyoto, Japan, in 1983, 1985, and 1988, respectively.

He is currently Director of Research at Home Wireless Networks, Norcross, GA. From 1988 to 1994, he was a Member of Technical Staff at Bellcore, Red Bank, NJ, conducting research on wireless communications systems and experimental prototyping of low-power radio links for personal communications. In 1994, he joined AT&T Bell Laboratories and continued to work in the area of wireless communications. His research interests have been in the areas of equalization, modulation, coding, CDMA and power control, and cellular system architectures and infrastructures. He holds 11 U.S. patents.

Dr. Ariyavisitakul is a member of the Institute of Electronics, Information, and Communication Engineers of Japan. He is currently Editor for Wireless Techniques and Fading for the IEEE TRANSACTIONS ON COMMUNICATIONS. He received the 1988 Niwa Memorial Award in Tokyo, Japan, for outstanding research and publication.

Jack H. Winters (S'77–M'81–SM'88–F'96) received the B.S.E.E. degree from the University of Cincinatti, Cincinnati, OH, in 1977 and the M.S. and Ph.D. degrees in electrical engineering from The Ohio State University, Columbus, in 1978 and 1981, respectively. Since 1981, he has been with AT&T Bell Laboratories and now AT&T Labs-Research, where is in the Wireless Systems Research Department. He has studied signal processing techniques for increasing the capacity and reducing signal distortion in fiber optic, mobile radio, and indoor radio systems and is currently studying adaptive arrays and equalization for indoor and mobile radio.

Dr. Winters is a member of Sigma Xi.

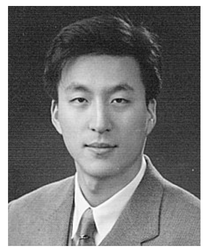

Inkyu Lee (S'92–M'95) was born in Seoul, Korea, in 1967. He received the B.S. degree (with honors) in control and instrumentation engineering from Seoul National University, Seoul, Korea, in 1990. He received the M.S. and Ph.D. degrees in electrical engineering from Stanford University, Stanford, CA, in 1992 and 1995, respectively.

From 1991 to 1995, he was a Research Assistant at the Information Systems Laboratory at Stanford University. In 1995, he joined AT&T Bell Laboratories. He is currently a Member of Technical Staff at Lucent Technologies, Bell Laboratories, Murray Hill, NJ. His research interests include digital communications, signal processing and coding techniques applied to wireless systems, digital subscriber lines, and magnetic recording channels. He is currently working on iterative decoding techniques.